CHALMERS
UNIVERSITY OF TECHNOLOGY

Experimental study of high-energy fission and quasi-fission dynamics with fusion-induced fission reactions at VAMOS(++)

Experimental study of high-energy fission and quasi-fission dynamics with fusion-induced fission reactions at VAMOS++

D. Fernández[1,*], *M. Caamaño*[1,**], *D. Ramos*[2,***], *A. Lemasson*[2], *M. Rejmund*[2], *H. Álvarez-Pol*[1], *L. Audouin*[3], *J. D. Frankland*[2], *B. Fernández-Domínguez*[1], *E. Galiana-Baldó*[4], *J. Piot*[2], *C. Schmitt*[5], *D. Ackermann*[2], *S. Biswas*[2], *E. Clement*[2], *D. Durand*[6], *F. Farget*[6], *M. O. Fregeau*[2], *D. Galaviz*[4], *A. Heinz*[7], *A. Henriques*[8], *B. Jacquot*[2], *B. Jurado*[8], *Y. H. Kim*[2], *P. Morfouace*[2], *D. Ralet*[9], *T. Roger*[2], *P. Teubig*[4], and *I. Tsekhanovich*[8]

[1]IGFAE – Universidad de Santiago de Compostela, E–15706 Santiago de Compostela, Spain
[2]GANIL, CEA/DRF-CNRS/IN2P3, BP 55027, F-14076 Caen Cedex 5, France
[3]IPN Orsay, Université de Paris-Saclay, CNRS/IN2P3, F-91406 Orsay Cedex, France
[4]LIP Lisboa, 1649-003 Lisbon, Portugal
[5]IPHC Strasbourg, Université de Strasbourg-CNRS/IN2P3, F-67037 Strasbourg Cedex 2, France
[6]LPC Caen, Université de Caen Basse-Normandie-ENSICAEN-CNRS/IN2P3, F-14050 Caen Cedex, France
[7]Department of Physics, Chalmers University of Technology, SE-41296 Göteborg, Sweden
[8]CENBG, IN2P3/CNRS-Université de Bordeaux, F-33175 Gradignan Cedex, France
[9]CSNSM, CNRS/IN2P3, Université de Paris-Saclay, F-91405 Orsay, France

Abstract. During the last decade, the use of inverse kinematics in the experimental study of fission is bringing a wealth of new observables obtained in single measurements, allowing their analysis and their correlations. An ongoing application of this technique is the basis of a series of experiments performed with the variable-mode, large-acceptance VAMOS++ spectrometer at GANIL. A recent experiment has been focused on the survival of the nuclear structure effects at high excitation energy in fission and quasi-fission. The full isotopic identification of fragments, the fission dynamics and the ratio between the production of fragments with even and odd atomic numbers, the so-called proton even-odd effect, are shown. The latter shows a different mechanism for fission and quasi-fission that could be used to separate fission from quasi-fission.

1 Introduction

Both fission and quasi-fission processes have similar final products. However, there are two remarkable differences between these processes. On the one hand, there is an equilibrated compound nucleus in fission but not in quasi-fission. On the other hand, quasi-fission is significantly faster than the fission process [1]. Experimental data aim to find observables to separate the two processes. The complete identification of fragments opens new possibilities, such as the relative production of even- and odd-Z fragments, the so-called even-odd effect.

In a previous experiment [2], fusion-induced fission of ^{250}Cf shows that structure effects may survive in the neutron-to-proton ratio of fragments and in the total kinetic energy, even at excitation energies of the order of 40 MeV.

In 2017, the E753 experiment was performed at GANIL using the VAMOS++ spectrometer to study the fission and quasi-fission processes also at high excitation energy, and analyse the survival of nuclear structure effects in both processes.

*e-mail: dani.fernandez@usc.es
**e-mail: manuel.fresco@usc.es
***e-mail: diego.ramos@ganil.fr

In this document the data of ^{265}Db from ^{238}U + ^{27}Al reaction are presented and discussed. The isotopic-fission yields $Y(Z,A)$, the elemental yields $Y(Z)$, the even-odd effect, the averaged velocity and the neutron evaporation are presented.

2 Experimental setup

VAMOS++ is a variable mode spectrometer [3, 4] composed of a large magnetic dipole and two quadrupoles, and a set of detectors at the focal plane that measure the energy, energy loss, the angles and positions of those particles that reach the end of the focal plane. The magnetic rigidity is reconstructed using those positions and the angles at focal plane. The velocity vector is measured at the target position, before the spectrometer. Regarding the fission fragments, the measured observables are: atomic number (Z), mass number (A), velocity vector, and kinetic energy. For the fissioning system, Z, A, and its excitation energy (E^*) are obtained [5].

The VAMOS++ angular acceptance is $\Delta\theta$=±7° and $\Delta\phi$=±10°. In this experiment, the spectrometer was used in two different settings of central magnetic rigidity ($B\rho_0$) and angle ($\theta_{\rm lab}$): $B\rho_0$=1.24 Tm, $\theta_{\rm lab}$=14° and $B\rho_0$=1.1 Tm, $\theta_{\rm lab}$ = 21.5°. Further details on VAMOS++ along with

typical performances for the fission-fragment detection are given in Refs. [6–8].

In this experiment, a ^{238}U beam at 5.9 *A*MeV impinged on four different light targets to generate different fissioning systems (FS) through transfer and fusion reactions. In the case of transfer or inelastic reactions, the target-like recoil is measured with a silicon telescope placed around the target. Fusion reactions are assumed when no recoil is detected. See [9] for more details. Once a FS is formed, it splits into two fission fragments (FF) and one of them is detected in VAMOS++. The targets used in the experiment were: 0.5 mg/cm^2 of ^{9}Be, 0.1 mg/cm^2 of ^{nat}B, 0.5 mg/cm^2 of ^{24}Mg, and 0.2 mg/cm^2 of ^{27}Al, that correspond to the following compound systems: ^{247}Cm, ^{249}Bk, ^{262}Rf, and ^{265}Db.

The advantage of using inverse kinematics is that it provides higher velocity to the FF that allows them to traverse several detector layers and to have access to a set of observables that cannot be achieved with direct kinematics.

3 Results with the aluminium target

Preliminary results from fusion–fission with the aluminium target are reported here. As previously mentioned, the compound produced is ^{265}Db with $E^* = 61.2$ MeV.

3.1 Fission yields

Isotopic-fission yields were derived, following the procedure presented in Refs. [10, 11]. The isotopic-fission yields are the result of counting the fission events, weighted by spectrometer acceptance, the angular and intrinsic efficiencies, the relative normalization between both settings ($\theta_{lab} = 14°$, $\theta_{lab} = 21.5°$) after the contamination subtraction of transfer-fission events.

The error bars represented in the data are the statistical uncertainties. The systematic uncertainties range from 2% in the heavier fragments up to 10% in the lighter ones.

Figure 1 shows the isotopic yields of ^{265}Db presented as a function of the fragment mass. Each color corresponds to one Z between Z=30 and Z=66. The resolution in the atomic number identification is $\Delta Z/Z \sim 1/80$, while in mass is $\Delta A/A \sim 1/200$.

The elemental yields $Y(Z)$ can be evaluated for each Z after summing the contribution of each mass: $Y(Z) = \sum_A Y(Z, A)$. The result is shown in Figure 2 together with the prediction of the semi-empirical code GEF [12] and a previous measurement [13] of a similar reaction. An approximation of the quasi-fission distribution, in solid blue line, resulting from the subtraction of the GEF simulation from the data.

The result shows a non-symmetric distribution of $Y(Z)$. This is explained with the restricted region of centre-of-mass (c.m.) angle covered in this experiment. As explained before, there is a strong correlation between the fragment mass and the c.m. angle. In this case, the experimental coverage only includes the heavy-fragment mass of quasi-fission, while the corresponding light fragments

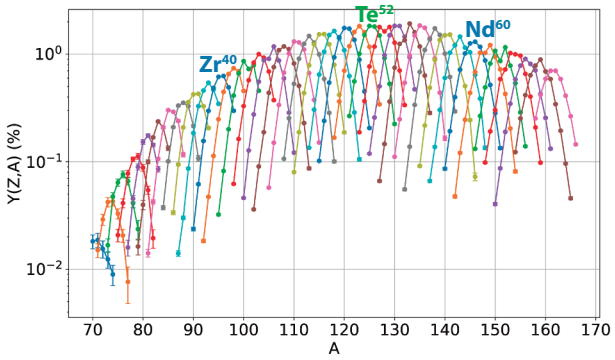

Figure 1. Isotopic fission yields $Y(Z, A)$ of fusion-induced fission of ^{265}Db at $E^* = 61.2$ MeV. Each colour line corresponds to one element. Zr^{40}, Te^{52}, and Nd^{60} are shown for reference.

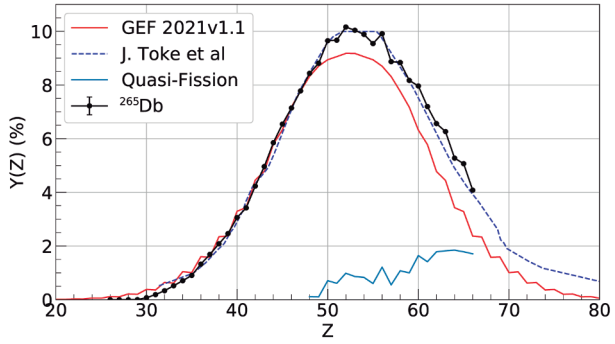

Figure 2. Elemental yield distribution $Y(Z)$ of fragments from ^{265}Db fusion-fission reactions (black points and solid black line) compared with the GEF prediction (red line) and previous measurement from [13] (dashed blue line). Quasi-fission approximated distribution extracted from the difference between data and GEF prediction (solid blue line).

would be in the complementary c.m. angle, not covered here. The $Y(Z)$ distribution is in agreement with the previous measurement [13], once the same restrictions are applied. The comparison with the GEF model [12] shows an agreement on the light-fragment part of the distribution. This is because the fission component of the reaction is not affected by the restriction in angular coverage. Taking this into account, the contribution of quasi-fission in the heavy region is determined as the excess of yields concerning to GEF.

3.2 Even-odd staggering in elemental yields

As stated, the current experimental setup provides access to more observables than previous measurements [13]. The elemental yields $Y(Z)$ allow to estimate the local even-odd effect δ of the fission fragments. This can be defined as the relative difference between the production of even-Z and odd-Z fragments measured. The even-odd effect is related with the energy dissipation and the transfer of protons between both fragments before scission. Although, there are a number of prescriptions, we have chosen the widely-used formula from Tracy et al. [14] to evaluate δ in

this work:

$$\delta(Z+1.5) = \frac{(-1)^Z}{8}\left(\ln(Y_0) - \ln(Y_3) + 3\left[\ln(Y_2) - \ln(Y_1)\right]\right),$$

where $Y_i \doteq Y(Z+i)$.

Figure 3 shows the experimental δ compared with the GEF prediction as a function of proton number of the fragments.

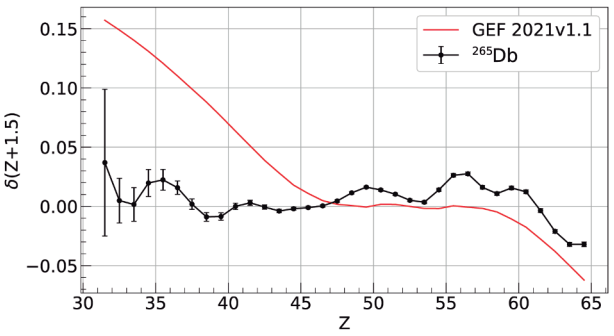

Figure 3. Measured even-odd effect δ (black points and line) compared with GEF (red line) as a function of Z.

According to previous measurements in ^{250}Cf [15], the even-odd effect is close to zero at $E^* \sim 40$ MeV. The large number of broken pairs is almost equally distributed between the fragments, resulting in a similar production of even- and odd-Z systems. The same beheaviour is expected in the experimental data at $E^* = 61.2$ MeV. Figure 3 shows and even-odd effect compatible with zero for the light fragments but not for the heavy ones.

This region with a non-zero delta coincides with the region where quasi-fission is identified in Figure 2, therefore is reasonable to assign this non-zero δ to the presence of quasi-fission. Concerning GEF, it seems to overestimate δ probably due to an overestimation of the pre-saddle neutron evaporation, which would reduce E^* in the fissioning system, and thus increase δ. This result also hints at δ as another observable able to separate fission from quasi-fission.

3.3 Fission dynamics

Since velocity and angles of fragments can be measured in the laboratory frame ($V_{\rm lab}$, $\theta_{\rm lab}$) as well as that of the fissioning system, the c.m. velocity of the fission fragments $V^{\rm FF}_{\rm c.m.}$ can be reconstructed on an event-by event basis, allowing the access the fission dynamics. Figure 4 shows $V^{\rm FF}_{\rm c.m.}$ as a function of the fragment A where each panel corresponds to one Z. The experimental data are in good agreement with GEF for $Z > 40$ but there is a deviation for the light fragments. This deviation is also seen in Figure 5, where the averaged velocity of the fragments is presented as a function of Z. Both figures show a slight overestimation of GEF prediction where the largest deviations appear for the more neutron-rich isotopes.

The fissioning system is excited and may emit neutrons before the saddle point, reducing the effective excitation energy before beginning the dynamical fission process. Information about these neutrons cannot be accessed with the present experimental setup. The GEF code predicts an average multiplicity of 2.4 pre-saddle neutrons. Also, while the system could emit neutrons on the path from the saddle to scission, reducing the excitation energy of the fission fragments, at the scission point the fragment still have large deformations and some intrinsic energy. This energy is mainly released by neutron evaporation from the fission fragments.

4 Conclusions

With the VAMOS++ setup, a collection of observables can be obtained, including the complete isotopic and elemental yields distributions. In this case, preliminary results of the ^{265}Db fissioning system are shown.

The elemental fission yields show a contribution corresponding to the quasi-fission process, and the odd-even effect for heavy fragments suggests a different mechanism of nucleon exchange between pre-fragments in quasi-fission. This observable seems to be a good candidate to separate both processes.

Finally, the isotopic velocity in the centre of mass frame of the fission fragments and the averaged velocity for each Z are shown. This will allow access to new observables of the fission dynamics, such as the total kinetic energy or the total excitation energy.

References

[1] D. J. Hinde, R. du Rietz, C. Simenel, M. Dasgupta, A. Wakhle, M. Evers, and D. H. Luong, AIP Conf. Proc. 1423, 65 (2012).

[2] M. Caamaño, F. Farget, O. Delaune, K. H. Schmidt, C. Schmitt, L. Audouin, C. O. Bacri, J. Benlliure, E. Casarejos, X. Derkx, B. Fernández-Domínguez, L. Gaudefroy, C. Golabek, B. Jurado, A. Lemasson, D. Ramos, C. Rodríguez-Tajes, T. Roger, and A. Shrivastava. Phys. Rev. C 92, 034606 (2015).

[3] S. Pullanhiotan, M. Rejmund, A. Navin, W. Mittig, S. Bhattacharyya, Nucl. Instr. and Meth. A 593, 343 (2008).

[4] M. Rejmund, B. Lecornu, A. Navin, C. Schmitt, S. Damoy, O. Delaune, J.M. Enguerrand, G. Fremont, P. Gangnant, L. Gaudefroy, et al., Nucl. Instr. and Meth. A 646, 184 (2008).

[5] C. Rodríguez-Tajes, F. Farget, X. Derkx, M. Caamaño, O. Delaune, K.-H. Schmidt, E. Clement, A. Dijon, A. Heinz, T. Roger, L. Audouin, J. Benlliure et al., Phys. Rev. C 89, 024614 (2014).

[6] M. Rejmund, B. Lecornu, A. Navin, C. Schmitt, S. Damoy, O. Delaune, J.M. Enguerrand, G. Fremont, P. Gangnant, L. Gaudefroy, B. Jacquot, J. Pancin et al., Nucl. Instr. and Meth. A 646, 184 (2011).

[7] M. Vandebrouck, A. Lemasson, M. Rejmund, G. Fremont, J. Pancin, A. Navin, C. Michelagnoli, J. Goupil, C. Spitaels, and B. Jacquot. Nucl. Instr. and Meth. A 812,112 (2016).

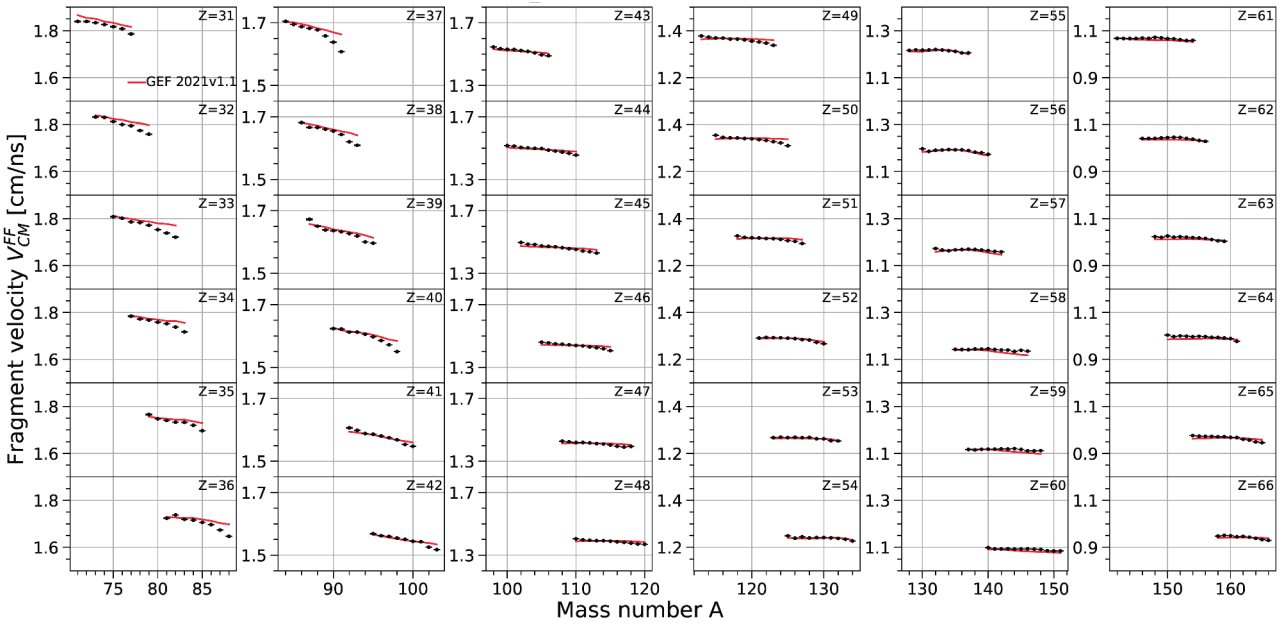

Figure 4. Each panel shows the centre of mass velocity as a function of A for the different elements produced in fusion-fission of ^{265}Db (black points). The GEF prediction is shown by the red lines.

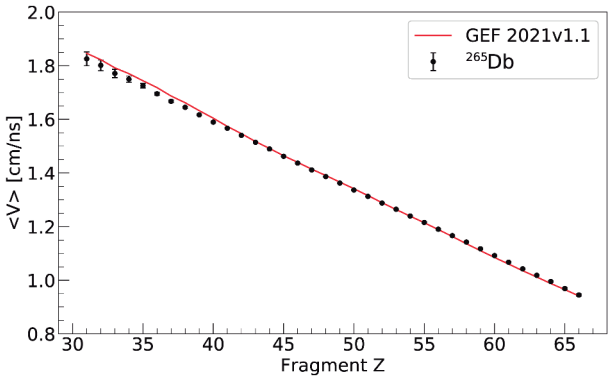

Figure 5. Average velocity $V_{\mathrm{c.m.}}^{\mathrm{FF}}$ as a function of Z (black points) compared with GEF (red line).

[8] Y. Kim, A. Lemasson, M. Rejmund, A. Navin, S. Biswas, C. Michelagnoli, I. Stefan, R. Banik, P. Bednarczyk, S. Bhattacharya, S. Bhattacharyya, E. Clement et al., Eur. Phys. J. A 53, 162 (2017).

[9] D. Ramos, M. Caamaño, A. Lemasson, M. Rejmund, L. Audouin, H. Álvarez-Pol, J. D. Frankland, B. Fernández-Domínguez, E. Galiana-Baldó, J. Piot, D. Ackermann, S. Biswas, E. Clement, D. Durand, F. Farget, M. O. Fregeau, D. Galaviz, A. Heinz, A. I. Henriques, B. Jacquot, B. Jurado, Y. H. Kim, P. Morfouace, D. Ralet, T. Roger, C. Schmitt, P. Teubig, and I. Tsekhanovich, Phys. Rev. L 123, 092503 (2019).

[10] M. Caamaño, O. Delaune, F. Farget, X. Derkx, K.-H. Schmidt, L. Audouin, C.-O. Bacri, G. Barreau, J. Benlliure, E. Casarejos, A. Chbihi, B. Fernández-Domínguez et al., Phys. Rev. C 88, 024605 (2013).

[11] D. Ramos, M. Caamaño, F. Farget, C. Rodríguez-Tajes, L. Audouin, J. Benlliure, E. Casarejos, E. Clement, D. Cortina, O. Delaune, X. Derkx, A. Dijon et al., Phys. Rev. C 97, 054612 (2018).

[12] K.-H. Schmidt, B. Jurado, C. Amouroux, and C. Schmitt, Nucl. Data Sheets 131, 107 (2016).

[13] J. Toke, R. Bock, G. X. Dai, A. Gobbi, S. Gralla, K. D. Hildenbrand, J. Kuzminski, W. F. J. Müller, A. Olmi, and H. Stelzer Nucl. Phys. A 440, 327 (1985).

[14] B. L. Tracy, J. Chaumont, R. Klapisch, J. M. Nitschke, A. M. Poskanzer, E. Roeckl, and C. Thibault. Phys. Rev. C 5, 222 (1972).

[15] D. Ramos, M. Caamaño, F. Farget, C. Rodríguez-Tajes, L. Audouin, J. Benlliure, E. Casarejos, E. Clement, D. Cortina, O. Delaune, et al. Phys. Rev. C 99, 024615 (2019).